BIOCHEMISTRY
including biophysical chemistry & molecular biology

Article

pubs.acs.org/biochemistry

Relationship between Conformational Stability and Amplification Efficiency of Prions

Nuria Gonzalez-Montalban,[†] Natallia Makarava,[†] Regina Savtchenko,[†] and Ilia V. Baskakov*[,†,‡]

[†]Center for Biomedical Engineering and Technology and [‡]Department of Anatomy and Neurobiology, University of Maryland School of Medicine, Baltimore, Maryland 21201, United States

Supporting Information

ABSTRACT: Recent studies demonstrated that the efficiency, rate, and yield of prion amplification *in vitro* could be substantially improved by supplementing protein misfolding cyclic amplification (PMCA) with Teflon beads [Gonzalez-Montalban et al. (2011) *PLoS Pathog.* 7, e1001277]. Here we employed the new PMCA format with beads (PMCAb) to gain insight into the mechanism of prion amplification. Using a panel of six hamster prion strains, the effect of beads on amplification was found to be strain-specific, with the largest improvements in efficiency observed for strains with the highest conformational stability. This result suggests a link between PrP^{Sc} conformational stability and its fragmentation rate and that beads improved amplification by assisting fragmentation. Furthermore, while exploring the PrP^{Sc}-independent bead effect mechanism, a synergy between the effects of RNA and beads on amplification was observed. Consistent with previous studies, amplification of all six hamster strains tested here was found to be RNA-dependent. Under sonication conditions used for PMCA, large RNA molecules were found to degrade into smaller fragments of a size that was previously shown to be the most effective in facilitating prion conversion. We speculate that sonication-induced changes in RNA size distribution could be one of the rate-limiting steps in prion amplification.

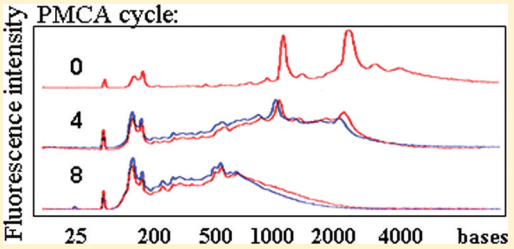

In the past 10 years, protein misfolding cyclic amplification (PMCA) has become an important tool in prion research.[1] A number of studies have provided strong evidence that fully infectious authentic prion structures can be generated *de novo* or amplified in PMCA.[2−4] When seeded with experimental prion strains, PMCA reactions preserve strain-specific features.[5,6] PMCA has been employed for elucidating cross-species transmission barriers,[6,7] studying strain adaptation and interference,[7,8] exploring cofactors involved in conversion,[9−12] investigating the role of prion protein glycosylation,[13] and developing prion detection assays.[14−17]

While the range of application of the PMCA technique has been expanding, the mechanism responsible for prion amplification remains hypothetical. PMCA consists of two alternating steps: sonication and incubation. The sonication step is presumably responsible for breaking large PrP^{Sc} particles into smaller fragments, whereas the incubation step is presumably required for the growth of small PrP^{Sc} particles through recruitment of PrP^{C} molecules.[1] The rate-limiting steps in prion amplification in PMCA and the reasons behind substantially different amplification rates for different prion strains remain unknown.

In previous studies, we found that prion amplification efficiency could be significantly improved by supplementing PMCA reactions with Teflon beads.[18] Because beads improve the rate and yield of prion conversion, identification of the reaction steps affected by beads can provide new information about the prion amplification mechanism. To explain the positive effect of beads, several hypothetical mechanisms have been proposed: (i) beads optimize the efficiency of PrP^{Sc} fragmentation; (ii) beads increase the accessibility and/or slowdown degradation of PrP^{C} during PMCA reactions; or (iii) beads increase the accessibility of cofactors, specifically, RNA. The current work utilizes PMCA with beads (PMCAb) for exploring the mechanism of prion amplification.

EXPERIMENTAL PROCEDURES

Reagents. A panel of six hamster prion strains was used: Hyper, ME7H, Drowsy, and 139H scrapie brain homogenates were kindly provided by Richard Bessen (Montana State University, Bozeman, MT); 263K and 10% NBH were kindly provided by Robert Rohwer (Veterans Affair Maryland Health Care System, Baltimore, MD); SSLOW scrapie brain homogenate was prepared using animals from the second passage of SSLOW with an incubation time to clinical disease 481 ± 4 days.[19] Teflon beads (2.38 mm diameter, McMaster-Carr, Los Angeles, CA) were used in all PMCAb reactions or sonication procedures.

Protein Misfolding Cyclic Amplification. Healthy hamsters were euthanized and immediately perfused with PBS, pH 7.4, supplemented with 5 mM EDTA. Brains were dissected, and 10% brain homogenate (w/v) was prepared using ice-cold conversion buffer and glass/Teflon tissue grinders cooled on ice and attached to a constant torque homogenizer (Heidolph RZR2020). The brains were ground at low speed until

Received: June 21, 2011
Revised: August 16, 2011
Published: August 17, 2011

homogeneous, and then five additional strokes completed the homogenization. The composition of conversion buffer was as previously described:[2] Ca^{2+}-free and Mg^{2+}-free PBS, pH 7.5, supplemented with 0.15 M NaCl, 1.0% Triton, and 1 tablet of Complete protease inhibitors cocktail (Roche, Cat. No. 1836145) per 50 mL of conversion buffer. The resulting 10% normal brain homogenate (NBH) in conversion buffer was used as the substrate in PMCA or PMCAb reactions. To prepare seeds, 10% scrapie brain homogenates in PBS were serially diluted 10^2−10^5-fold, as indicated, in the conversion buffer, and 10 μL of the dilution was used to seed amplification in 90 μL of NBH. Samples in 0.2 mL thin-wall PCR tubes (Fisher, Cat. No. 14230205) were placed in a floating rack inside a Misonix S-4000 microplate horn filled with 350 mL of water. Two coils of rubber tubing attached to a circulating water bath were installed to maintain 37 °C inside the sonicator chamber. The standard sonication program consisted of 30 s sonication pulses delivered at 50−60% power efficiency applied every 30 min during a 24 h period. For PMCAb three Teflon beads were placed into the 0.2 mL tubes first, and then NBH and seeds were added. To analyze PMCA or PMCAb products, 15 μL of each sample was supplemented with 2.5 μL of SDS and 2.5 μL of proteinase K (PK), to a final concentration of SDS and PK of 0.25% and 50 μg/mL, respectively, followed by incubation at 37 °C for 1 h. The digestion was terminated by addition of SDS-sample buffer and incubated for 10 min at 100 °C. Samples were loaded onto NuPAGE 12% BisTris gels, transferred to PVDF membrane, and stained with 3F4 antibody, and the Western blot was developed with a Supersignal West Pico Chemiluminescent Substrate kit (Thermo Scientific, Rockford, IL).

Analysis of Conformational Stability. 10% brain homogenates were diluted 10 times into conversion buffer, then supplemented with an equal volume of GdnHCl solution in PBS to a final concentration of GdnHCl ranging from 0.4 to 4 M, and incubated at room temperature for 1 h. Next, nine volumes of 2% sarkosyl in PBS were added to all samples followed by 1 h incubation at room temperature, and then the samples were treated with 20 μg/mL PK for 1 h at 37 °C with shaking. The digestion was stopped by 2 mM PMSF, and the proteins were precipitated in four volumes of ice-cold acetone, overnight incubation at −20 °C, and subsequent 30 min centrifugation at 16000*g*. Pellets were dried for 30 min, resuspended in 1×SDS-sample buffer, loaded into NuPAGE 12% bisTris gels, then transferred to PVDF membrane, and stained with 3F4 antibody.

Preparation of RNA-Depleted Normal Brain Homogenate. 50 μL of 10 mg/mL RNase A (Sigma, Cat. No. R4875) was added to 5 mL of 10% Syrian hamster NBH to a final RNase concentration of 100 μg/mL. To prepare mock-digested NBH, 50 μL of RNA-free water was added to 5 mL of 10% NBH. Both mixtures were incubated at 37 °C for 1 h under gentle rotation; then total RNA was purified and analyzed using gel electrophoresis as described below.

Purification of Total RNA and RNA Analysis. The fresh livers of C57 mice were stored at 4 °C overnight in 10 V of RNAlater Solution (Ambion, Cat. No. AM7020) to allow the solution to penetrate the liver tissue and protect RNA from degradation. Then supernatant was removed, and livers were store at −80 °C. For purification livers were taken out from −80 °C, quickly wiped to remove the excess of RNAlater, and homogenized in 10 V of TRI Reagent Solution (Ambion, Cat. No. AM9738), and total RNA was purified according to the manufacturer's procedure. Purified RNA was diluted with DEPC-treated RNase free water to a final concentration of 500 μg/mL and subjected to a sonication procedure identical to that used in PMCA (30 s sonication pulses applied every 30 min during a 24 h period). For the analysis of RNA fragmentation, gel electrophoresis was performed using 1.2% agarose gel in TBE buffer; each lane was loaded with 6 μg of RNA. As an alternative method, the Agilent 2100 Bioanalyzer and the Agilent RNA 6000 Nano Kit were used according to the manufacturer's procedure (Agilent Technologies, CA). To avoid RNA degradation due to possible contamination, plastic tubes, beads, and tweezers were treated with 1% DEPC for 2 h at 37 °C and then autoclaved.

RESULTS

Effect of Beads Is Strain-Specific. To test whether the effect of beads in improving the amplification efficiency is generic, we employed a panel of hamster strains with a broad range of conformational stabilities including 263K, Hyper (HY), SSLOW, ME7H, Drowsy (DY), and 139H (Figure 1).

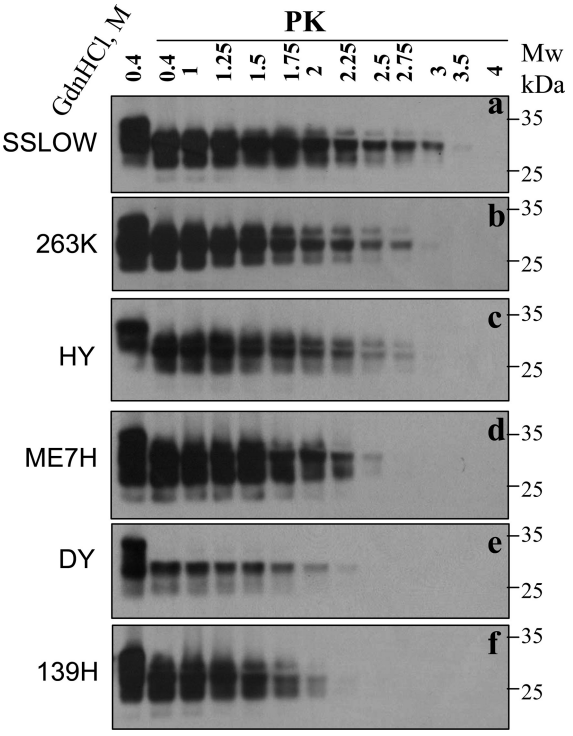

Figure 1. Analysis of conformational stability of six hamster strains. Scrapie brain homogenate from animals inoculated with SSLOW (a), 263K (b), HY (c), ME7H (d), DY (e), or 139H (f) was incubated with increasing concentrations of GdnHCl from 0.4 to 4 M for 1 h, then diluted out of GdnHCl, and digested with PK. Undigested brain material exposed to 0.4 M GdnHCl is provided as a reference.

Each strain was subjected to two PMCA rounds in the absence or presence of beads using three seed dilutions (Figure 2). Three serial seed dilutions were used because of individual strain-specific differences in amplification sensitivity and because beads were previously found to be most effective at high seed dilutions.[18] This experiment revealed the following rank order with respect to the impact of beads on improving the efficiency of amplification (starting from a strain for which beads had the highest impact): 263K > SSLOW > HY > ME7H

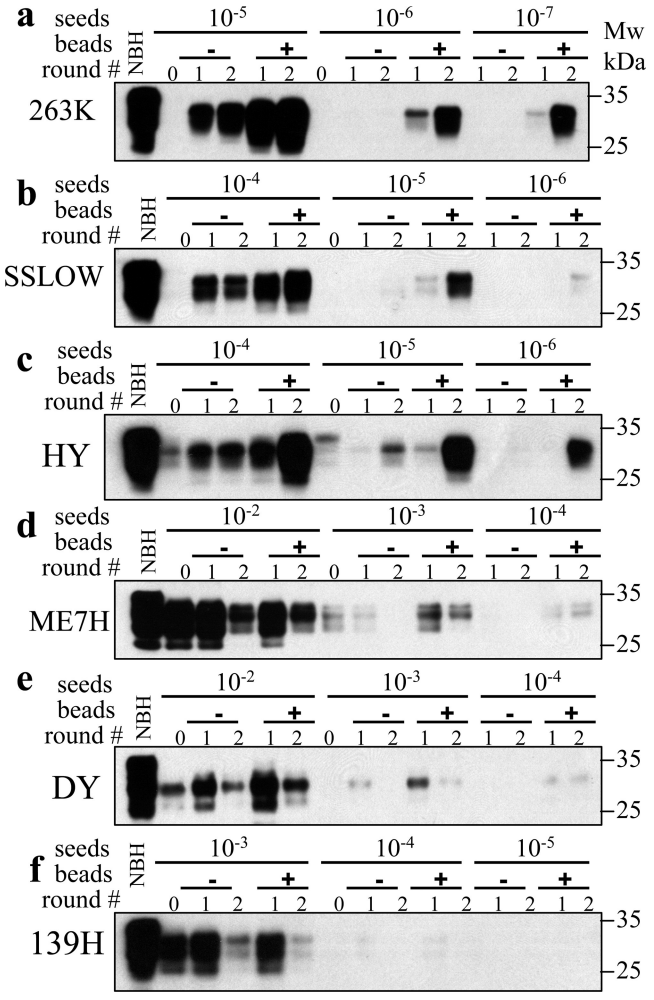

Figure 2. Effect of beads on amplification of six hamster strains. 263K (a), SSLOW (b), HY (c), ME7H (d), DY (e), or 139H (f) scrapie brain materials were diluted 10^2–10^7-fold into 10% NBH as indicated and subjected to two serial PMCA rounds in the absence or presence of beads. The material amplified in the first round was diluted 10-fold into 10% NBH for the second round. Prior to electrophoresis, samples were digested with PK. Undigested 10% NBH is provided as a reference.

≈ DY > 139H (Figure 2a–f). Beads were found to have the largest effect on amplification of 263K, HY, and SSLOW, a mild effect on amplification of ME7H and DY, and no detectible improvement on 139H (Figure 1f).

Correlation between PrP^{Sc} Conformational Stability and the Impact of Beads on Amplification Efficiency. To test whether the strain-specific differences in efficiency of beads is attributed to differences in PrP^{Sc} physical properties, conformational stability and strain-specific amplification rates were analyzed for the six hamster strains listed above. Consistent with previous studies, the conformational stability assay showed that SSLOW, 263K, and HY were the most stable strains, ME7H was moderately stable, while DY and 139H were the least stable strains (Figure 1). The highest improvements in amplification efficiency were observed for the strains with the highest conformational stability, whereas the strains with low stability showed very minor or no improvement in amplification rate. Taken together, these results support the hypothesis that beads facilitate fragmentation of PrP^{Sc}.

To establish strain-specific amplification rates, a set of serial PMCAb (sPMCAb) reactions were conducted for each strain with the dilution factors between serial rounds ranging from 1:3 to 1:1000 (Figure 3). The amplification rate is defined

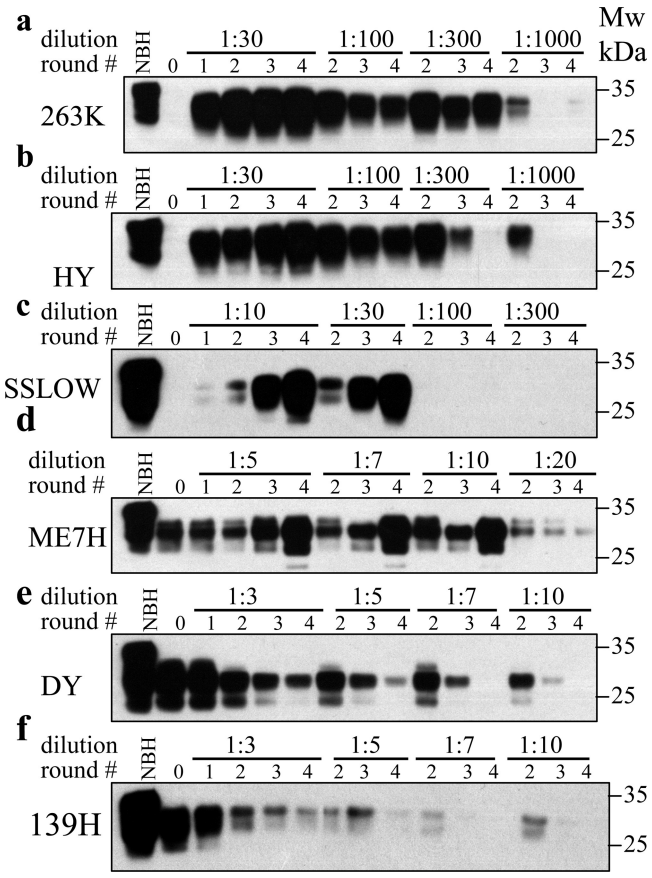

Figure 3. Analysis of PrP^{Sc} amplification fold. Scrapie brain materials were diluted 10^4-fold for 263K (a), HY (b), or SSLOW (c), 10^3-fold for ME7H (d), or 10^2-fold for DY (e) or 139H (f) into 10% NBH and subjected to four serial PMCAb rounds. The material amplified in each round was diluted 3-, 5-, 7-, 10-, 20-, 30-, 100-, 300-, or 1000-fold into 10% NBH for the next PMCA round, as indicated. Prior to electrophoresis, samples were digested with PK. Undigested 10% NBH is provided as a reference.

operationally as the highest dilution between serial PMCAb rounds at which amplification is still capable of compensating the effect of dilution, i.e., the highest dilution at which a strain can be maintained steadily. For instance, the amount of 263K PK-resistant material remained stable in sPMCAb at a 1:300 dilution but decayed at a 1:1000 dilution (Figure 3a); therefore, the amplification rate of 263K was determined to be 300. This experiment established the following rank order with respect to PMCAb amplification rates (starting from a strain with the highest rate): 263K > HY > SSLOW > ME7H > DY > 139H (Figure 3a–f). This experiment also revealed a relatively good correlation between strain-specific amplification rates and their conformational stability. The strains with the lowest stability (DY and 139H) displayed the poorest amplification rate, while the strains with high amplification rates (263K, HY, and SSLOW) were the most stable.

A Synergy between Effects of Beads and RNA. To test whether the effect of beads is mediated by mechanisms independent of PrP^{Sc} fragmentation, normal brain homogenate

dx.doi.org/10.1021/bi200950v | Biochemistry 2011, 50, 7933–7940

(NBH) was subjected to 48 cycles of sonication (an equivalent of one PMCA round) in the presence or absence of beads and used as a source of PrP^C in PMCA (Figure 4). PMCAs with

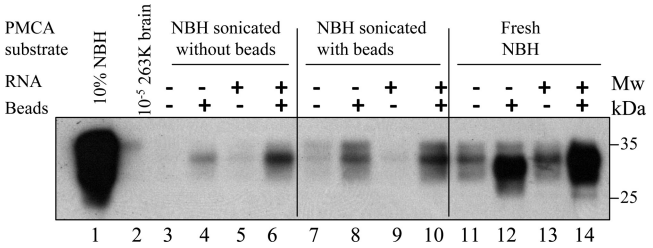

Figure 4. Synergy between effects of beads and RNA. 263K scrapie brain material was diluted 10^5-fold (lane 2) into NBH presonicated without beads (lanes 3–6), NBH presonicated with three beads (lanes 7–10), or fresh NBH (lanes 11–14) and subjected to a single PMCA round in the absence or presence of beads as indicated. Total mouse liver RNA was added to PMCA reactions as indicated. Prior to electrophoresis, samples were digested with PK. Undigested 10% NBH was provided as a reference (lane 1).

presonicated NBH were conducted in the presence or absence of beads. Sonication of NBH prior to PMCA reduced the conversion yield (compare lanes 3 and 4 to 11 and 12, respectively, in Figure 4). While the presence of beads during presonication of NBH partially restored the yield (compare lanes 7 and 8 to 3 and 4, respectively, in Figure 4), the yield did not reach the levels observed with fresh NBH (compare lanes 7 and 8 to 11 and 12, respectively, in Figure 4). Therefore, (i) NBH was no longer suitable for PMCA, after it was subjected to sonication cycles for 24 h, and (ii) the presence of beads during sonication of NBH prior to PMCA had minimal if any effects.

To test whether the negative effect of NBH presonication could be eliminated by adding extra RNA, total liver RNA was added to PMCA reactions. In the absence of beads in PMCA reactions, supplementing RNA showed no notable improvements (compare lane 5 to 3, lane 9 to 7, or line 13 to 11 in Figure 4). However, adding RNA to the reactions conducted with beads improved the conversion yield (compare lane 6 to 4, lane 10 to 8, or lane 14 to 12 in Figure 4). Similarly, addition of extra RNA to fresh NBH showed no notable improvement (compare lane 13 to 11 in Figure 4) unless beads were present during PMCA (compare lane 14 to lanes 13 and 11 in Figure 4). Thus, in the presence of extra RNA the improvements in yield were observed regardless of whether presonicated or fresh NBH was used. While in the absence of extra RNA beads improved the efficiency of conversion too (compare lane 12 to 11, lane 8 to 7, and lane 4 to 3 in Figure 4), these improvements were less substantial than those observed in the presence of beads and extra RNA. These modest improvements could be due to the effect of beads on the RNA present in NBH.

Taken together, these results pointed to a synergy between RNA and beads and illustrated that both beads and RNA must be present during PMCA to have the optimal effect. To explore the synergetic effects of RNA and beads further, PMCA reactions were conducted using RNA-depleted NBH in the absence or presence of beads (Figure 5). Treatment of NBH with RNase for 1 h was found to effectively remove RNAs (Figure S1). As predicted, neither the presence of RNA (lanes 9 and 10 in Figure 5)) nor beads (lanes 5 and 6 in Figure 5))

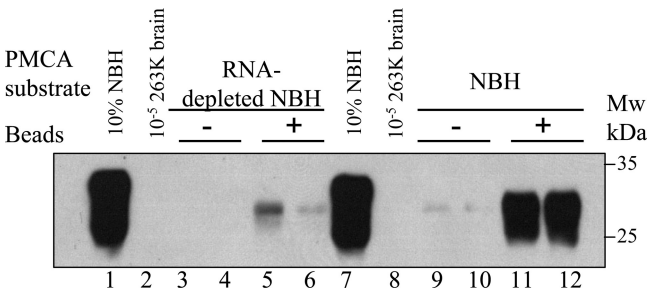

Figure 5. Effect of RNA-depletion on RNA-amplification. 263K scrapie brain material was diluted 10^5-fold (lanes 2 or 8) into RNA-depleted NBH (lanes 3–6) or NBH (lanes 9–12) and subjected to a single PMCA round in the absence or presence of beads as indicated. Prior to electrophoresis, samples were digested with PK. Undigested 10% NBH were provided as a reference (lanes 1 or 7). Amplification in two independent PMCA reactions is shown for each condition.

could guarantee an efficient amplification. However, in the presence of both RNA and beads, the yield of amplification increased significantly (lanes 11 and 12 in Figure 5). This experiment provided further support that beads and RNA had a synergistic effect on amplification.

RNA Dependency of Amplification of Hamster Strains. Considering the results from the previous experiments, one can presume that strain-specific differences in the effect of beads could be attributed in part to the differences in RNA dependency in strain amplification. Toward this question, we tested whether amplification of six hamster strains depended on RNA. Serial PMCAb reactions were conducted in NBH or in RNA-depleted NBH (Figure 6). Four PMCAb rounds were performed for each condition to ensure that small amounts of RNA in the seed material did not affect the results in RNA-depleted NBH. Because of strain-specific differences in amplification rates, the dilution factors between serial rounds were adjusted individually for each strain based on the results of previous experiment. Higher dilutions were used for strains with higher amplification rates.

In the absence of RNA, the amplification was suppressed for all strains (Figure 6a–f). However, in RNA-depleted NBH, DY and 139H showed positive signals up to the third PMCAb round (Figure 6e,f). High amounts of seeds and a very low 1:5 dilution factor between serial PMCAb rounds could account for the signal in the second and third rounds in these two strains. The control experiments with a simple 1:5 serial dilution of seeds in the absence of a substrate showed the same decay rates as those observed during serial PMCA in RNA-depleted NBH (Figure 6e,f). This result confirmed that the signal observed in the second and third rounds for DY or 139H was simply due to seed dilution but not amplification. Therefore, in agreement with the previous studies,[3,9–11,20] this experiment revealed that amplification of all hamster strains tested (263K, HY, SSLOW, ME7H, DY, and 139H) was dependent on RNA. Unfortunately, due to intrinsically low amplification rates for the strains with low conformational stability, establishing the ranking order of strain amplification with respect to their RNA dependency is not feasible.

Sonication Fragments RNA. Previous studies illustrated that RNAs of sizes above 200 base pairs were the most effective in stimulating prion conversion in PMCA.[11,20] To explore the mechanisms behind RNA-stimulated prion conversion further, we tested whether sonication changes the RNA size distribution during PMCA. Total liver RNA was subjected to 48 sonication

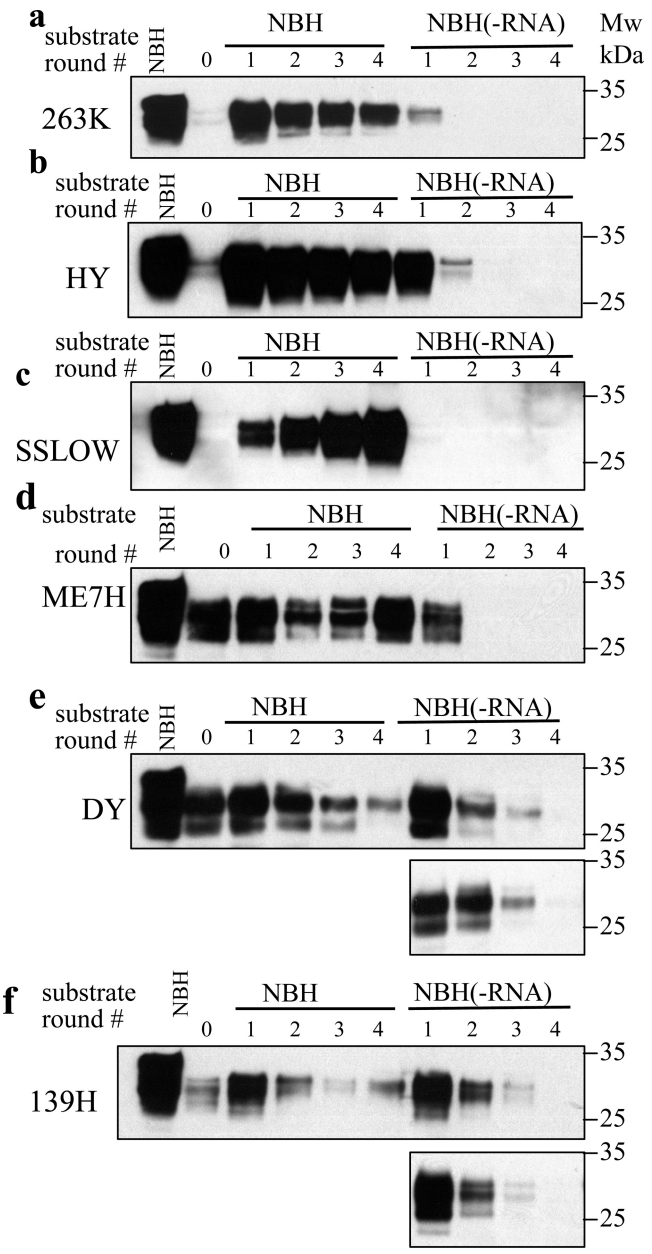

Figure 6. Analysis of RNA dependency of prion amplification. Scrapie brain materials were diluted 10^4-fold for 263K (a), HY (b), or SSLOW (c), 10^3-fold for ME7H (d), and 10^2-fold for DY (e) or 139H (f) into 10% NBH or RNA-ablated NBH (referred to as NBH(-RNA)) as indicated and subjected to four serial PMCAb rounds. The material amplified in each round was diluted 300-fold for 263K, 100-fold for HY, 10-fold for SSLOW or ME7H, and 5-fold for DY or139H for the next PMCAb round. Prior to electrophoresis, samples were digested with PK. Undigested 10% NBH is provided as a reference. The lower panels in (e) and (f) represent the results of serial 1:5 dilution of DY and 139H seeds, respectively, in the absence of amplification.

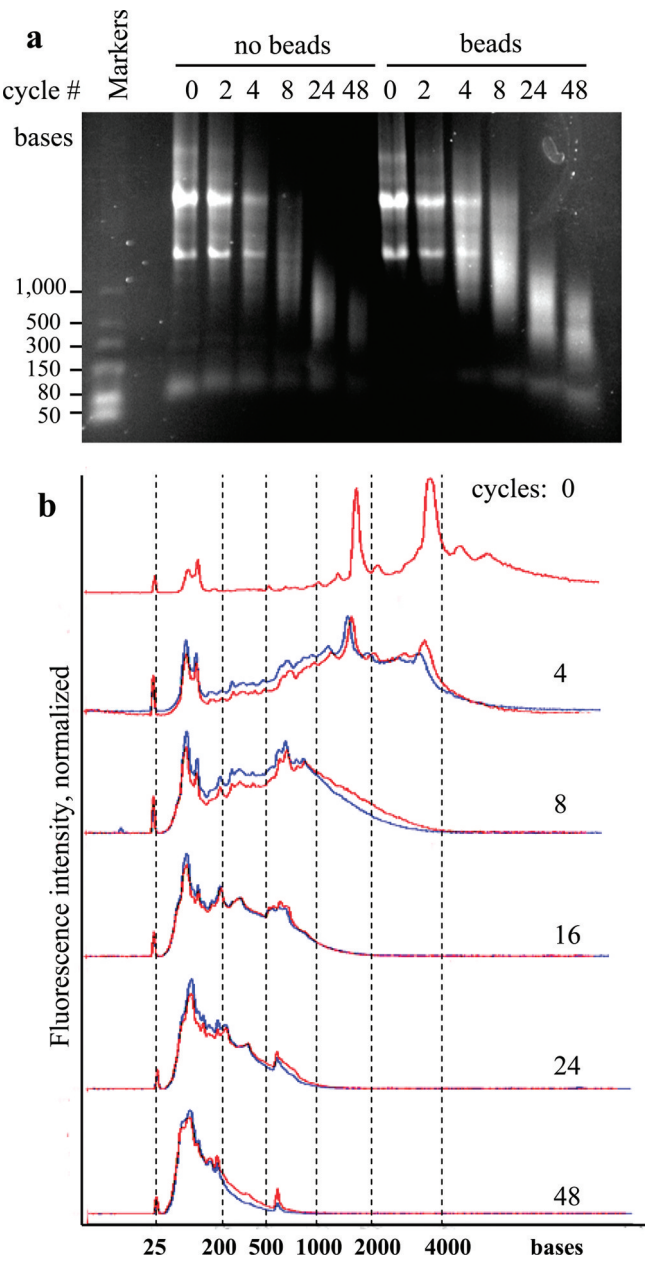

Figure 7. Analysis of RNA fragmentation. Total liver RNA was subjected to a sonication procedure identical to the one employed in PMCA (30 s sonication pulses applied every 30 min during a 24 h period) in the presence (blue lines) or absence of beads (red lines) as indicated. RNA size distribution was analyzed as a function of sonication cycle number by agarose gel (a) or microfluidic technology (b).

cycles, and the size distribution was analyzed as a function of sonication cycle using agarose gel electrophoresis or microfluidics-based technology using an Agilent 2100 Bioanalyzer. Both approaches revealed a gradual decrease in size of RNA as a function of sonication cycle number (Figure 7a,b). Before sonication, the profile of total RNA was dominated by two major bands at ~1.8 and 3.6 kbases that correspond to 18S and 28S rRNAs, respectively. By the eighth cycle, substantial amounts of RNAs were observed within 200−1000 base range (Figure 7b). At the 48th cycle, most of RNA molecules were found within the 50−200 base range (Figure 7b). The experiment was repeated several times and produced consistent results. No notable differences with respect to fragmentation kinetics or fragment size distribution were observed between RNA samples sonicated in the presence or absence of beads. While this experiment failed to explain the synergy between beads and RNA, it revealed that under the sonication conditions employed for PMCA, by the eighth cycle large RNA molecules were degraded into smaller fragments within a size range that was previously shown to be the most effective in stimulating prion conversion.[11,20] The same experiment

dx.doi.org/10.1021/bi200950v | Biochemistry 2011, 50, 7933−7940

showed that by the 48th cycle, the RNA was largely degraded into a size range previously shown to be too small to be effective in facilitating prion conversion.[11,20]

DISCUSSION

Amplification of prions in PMCA is believed to involve two main steps: fragmentation of PrP^{Sc} particles and their growth. To date, the mechanism of amplification remains hypothetical. It is not known whether the amplification rate is limited by PrP^{Sc} fragmentation or binding and conversion of PrP^{C} into PrP^{Sc}. Furthermore, the extent to which degradation of PrP^{C} and/or PrP^{Sc} limits the amplification rate and the extent to which the amounts and availability of cellular cofactors impact the reaction also remain to be established. For a number of technical reasons, direct measurement of PrP^{Sc} size distribution during PMCA sonication cycles is very challenging and might not be informative. For instance, assuming that a PMCA round which consisted of 48 cycles amplifies PrP^{Sc} by ~10-fold, simple mathematical calculation shows that, on average, only 5 out of 100 PrP^{Sc} particles fragment in each sonication cycle, producing two particles from one.

The current work revealed several important findings that provide new insight into prion replication mechanisms. The largest improvements in the amplification with beads were observed for strains with the highest conformational stability. This result supports the notion that conformational stability controls the PrP^{Sc} fragmentation rate and that beads assist in fragmentation.[18] Alternatively, this result is also consistent with the view that conformationally stable strains are prone to form large PrP^{Sc} aggregates and, therefore, require bead assistance to break up aggregates during amplification. In previous studies, a correlation between conformational stability and incubation time to disease was observed for hamster and mouse synthetic prions generated in animals by inoculating recombinant PrP fibrils.[19,21,22] Shortening of the incubation time to disease observed during serial transmission of synthetic strains was found to coincide with a decrease in their conformational stability.[19,22] Furthermore, a strong correlation between the incubation time to disease and PrP^{Sc} conformational stability was also observed for a broad range of synthetic strains produced by inoculating recombinant PrP fibrils of various stability.[21] *In vitro* studies with recombinant PrP fibrils showed that amyloid structures with lower conformational stability produce smaller particles when fragmented by sonication than the amyloid fibrils of higher stability.[23] Taken together, these results support the hypothesis that PrP^{Sc} conformational stability is one of the factors that controls the incubation time to disease and that the PrP^{Sc} fragmentation rate presumably links the stability to the incubation time. Notably, previous studies on cross-species transmission of hamster-adapted strains suggested that PrP^{Sc} conformational stability also influences the transmission efficiency of prions between species.[24]

The linear relationship between conformational stability and incubation time did not hold if a broad group of hamster-adapted strains with diverse biological properties was considered.[25] The study by Ayers et al. suggested that other features such as strain-specific differences in neurotropism and cell tropism as well as involvement of astrocytes and microglia impact the rate of disease progression to a larger extent than PrP^{Sc} conformational stability.[25] It is possible that the incubation time to disease does not depend on the PrP^{Sc} accumulation rate as much as it reflects the strain-specific intrinsic neurotoxicity of PrP^{Sc}. For instance, some PrP^{Sc} strains or amyloid structures might be intrinsically more neurotoxic than other structures.[26,27] The precise relationship between strain-specific PrP^{Sc} structures and their neurotoxicity has yet to be established.

Consistent with the previous studies,[25] the strains with long incubation time to disease (139H, DY, and ME7H), with an exception of SSLOW, had very low amplification rates in PMCAb. Considering that SSLOW is characterized by a very slow progression of clinical disease in addition to long incubation time, the unique biological properties of this synthetic strain might account for its exceptional position. One can speculate that low amplification rates for 139H, DY, and ME7H could be due to their fast degradation rate rather than slow amplification per se, a hypothesis that needs to be tested in future studies. Low conformational stability of 139H, DY, and ME7H is consistent with this hypothesis. Taking into account all data available to date, the relationship between the incubation time to disease and conformational stability could be described by a biphasic rather than a linear curve. According to this model, the strains that have the shortest incubation time (263K or HY) are those for which the conformational properties are optimized to avoid rapid cell clearance while providing fast amplification. The strains with conformational stabilities lower than optimal (139H, DY, and ME7H) or higher than optimal (synthetic strains) exhibit long incubation times because of their high clearance rates or lower than optimal amplification rates, respectively.

Consistent with the previous studies,[9−11] amplification of all hamster strains tested here was found to be RNA-dependent. Whether or not RNA serves as a cofactor for prion replication in a cell is currently not known.[9,10,28] One could envision that ribophagy (authophagy of rRNAs[29]) supplies RNA fragments for prion conversion in the cellular compartments (autophagosomes or lysosomes) where PrP^{Sc} replication might take place. Unexpectedly, under PMCA sonication conditions, large RNA molecules were found to degrade into smaller fragments, producing a size distribution that was previously shown to be the most efficient in facilitating prion conversion.[11,20] Considering that multiple sonication cycles were required for generating RNAs of the most active sizes, one can speculate that sonication-induced fragmentation of RNA might represent one of the rate-limiting steps in prion amplification *in vitro*. However, by the 48th sonication cycle, most of the RNA was found to be degraded to fragments within the 50−200 bases range. Because RNAs of this size were previously shown to be not very effective in facilitating amplification,[11] further increase in the number of PMCAb cycles might not be productive for amplification of strains that rely on RNA. Taken together, these data suggest that the most productive time window for amplification of RNA-dependent strains in PMCAb could be only between cycles 8 and 24.

The current study revealed a synergy between the effects of beads and RNA on PrP^{Sc} amplification. The mechanism responsible for this synergistic effect has yet to be explored. The kinetics of sonication-induced RNA fragmentation was not affected by beads (Figure 7). We do not know whether beads alter accessibility of RNAs and/or change its secondary structure. Nevertheless, when all experiments on beads and RNA are considered together, the strongest effect of RNA in stimulating amplification was observed when beads were present in PMCA reactions and when RNA fragmentation occurred in parallel but not prior to the conversion. Because

polymeric cofactors of different biochemical natures might be involved in amplification of strains from different species,[10,16,30] the effect of sonication and beads on size distribution of these polymers have to be considered. Future optimization of PMCA conditions for slow-replicating strains might involve finding the right balance for effective fragmentation of PrP^{Sc} and a cofactor, while avoiding degradation of PrP^{Sc}.

■ ASSOCIATED CONTENT

Supporting Information

Analysis of RNA content in RNA-depleted NBH (Figure S1). This material is available free of charge via the Internet at http://pubs.acs.org.

■ AUTHOR INFORMATION

Corresponding Author

*Phone: 410-706-4562. Fax: 410-706-8184. E-mail: Baskakov@umaryland.edu.

Funding

This work was supported by NIH grant NS045585 to (I.V.B.) and by a Beatriu de Pinós Fellowship with the support of the Commission for Universities and Research of the Department of Innovation, Universities and Enterprise of the Government of Catalonia to (N.G.M).

■ ACKNOWLEDGMENTS

We thank Pamela Wright for editing the manuscript.

■ ABBREVIATIONS

PMCA, protein misfolding cyclic amplification; PMCAb, PMCA with Teflon beads; sPMCAb, serial PMCAb; PrP^{C}, normal cellular isoform of the prion protein; PrP^{Sc}, infectious, disease-related isoform of the prion protein; NBH, normal brain homogenate; HY, Hyper strain; DY, Drowsy strain; PK, proteinase K.

■ REFERENCES

(1) Saborio, G. P., Permanne, B., and Soto, C. (2001) Sensitive detection of pathological prion protein by cyclic amplification of protein misfolding. *Nature 411*, 810−813.

(2) Castilla, J., Saa, P., Hetz, C., and Soto, C. (2005) In vitro generation of infectious scrapie prions. *Cell 121*, 195−206.

(3) Deleault, N. R., Harris, B. T., Rees, J. R., and Supattapone, S. (2007) Formation of native prions from minimal components in vitro. *Proc. Acad. Natl. Sci. U. S. A. 104*, 9741−9746.

(4) Wang, F., Wang, X., Yuan, C.-G., and Ma, J. (2010) Generating a Prion Bacterially Expressed Recombinant Prion Protein. *Science 327*, 1132−1135.

(5) Castilla, J., Morales, R., Saa, P., Barria, M., Gambetti, P., and Soto, C. (2008) Cell-free propagation of prion strains. *EMBO J. 27*, 2557−2566.

(6) Green, K. M., Castilla, J., Seward, T. S., Napier, D. L., Jewell, J. E., Soto, C., and Telling, G. C. (2008) Accelerated High Fidelity Prion Amplification Within and Across Prion Species Barriers. *PLOS Pathog. 4*, e1000139.

(7) Castilla, J., Gonzalez-Romero, D., Saa, P., Morales, R., De Castro, J., and Soto, C. (2008) Crossing the Species Barrier by PrPSc Replication In Vitro Generates Unique Infectious Prions. *Cell 134*, 757−768.

(8) Shikiya, R. A., Ayers, J. I., Schutt, C. R., Kincaid, A. E., and Bartz, J. C. (2010) Coinfecting prion strains compete for a limiting cellular resource. *J. Virol. 84*, 5706−5714.

(9) Deleault, N. R., Lucassen, R. W., and Supattapone, S. (2003) RNA molecules stimulate prion protein conversion. *Nature 425*, 717−720.

(10) Deleault, N. R., Kascsak, R., Geoghegan, J. C., and Supattapone, S. (2010) Species-dependent differences in cofactor utilization for formation of the protease-resistant prion protein in vitro. *Biochemistry 49*, 3928−3934.

(11) Deleault, N. R., Geoghegan, J. C., Nishina, K., Kascsak, R., Williamson, R. A., and Supattapone, S. (2005) Protease-resistant Prion Protein Amplification Reconstituted with Partially Purified substrates and Synthetic Polyanions. *J. Biol. Chem. 280*, 26873−26879.

(12) Mays, C. E., and Ryou, C. (2010) Plasminogen stimulates propagation of protease-resistant prion protein *in vitro*. *FASEB J. 24*, 5102−5112.

(13) Nishina, K., Deleault, N. R., Mahal, S., Baskakov, I., Luhrs, T., Riek, R., and Supattapone, S. (2006) The Stoichiometry of Host PrPC Glycoforms Modulates the Efficiency of PrPSc formation in vitro. *Biochemistry 45*, 14129−14139.

(14) Saa, P., Castilla, J., and Soto, C. (2006) Presymptomatic Detection of Prions in Blood. *Science 313*, 92−94.

(15) Tattum, M. H., Jones, S., Pal, S., Collinge, J., and Jackson, G. S. (2010) Discrimination between prion-infected and normal blood samples by protein misfolding cyclic amplification. *Transfusion 50*, 2619−2627.

(16) Murayama, Y., Yoshioka, M., Masujin, K., Okada, H., Iwamaru, Y., Imamura, M., Matsuura, Y., Fukuda, S., Onoe, S., Yokoyama, T., and Mohri, S. (2010) Sulfated dextrans enhance in vitro amplification of bovine spongiform encephalopathy PrP(Sc) and enable ultra-sensitive detection of bovine PrP(Sc). *PLoS One 5*, e13152.

(17) Pritzkow, S., Wagenfuhr, K., Daus, M. L., Boerner, S., Lemmer, K., Thomzig, A., Mielke, M., and Beekes, M. (2011) Quantitative detection and biological propagation of scrapie seeding activity in vitro facilitate use of prions as model pathogens for disinfection. *PLoS One 6*, e20384.

(18) Gonzalez-Montalban, N., Makarava, N., Ostapchenko, V. G., Savtchenko, R., Alexeeva, I., Rohwer, R. G., and Baskakov, I. V. (2011) Highly Efficient Protein Misfolding Cyclic Amplification. *PLoS Pathogen 7*, e1001277.

(19) Makarava, N., Kovacs, G. G., Bocharova, O. V., Savtchenko, R., Alexeeva, I., Budka, H., Rohwer, R. G., and Baskakov, I. V. (2010) Recombinant prion protein induces a new transmissible prion disease in wild type animals. *Acta Neuropathol. 119*, 177−187.

(20) Geoghegan, J. C., Valdes, P. A., Orem, N. R., Deleault, N. R., Williamson, R. A., Harris, B. T., and Supattapone, S. (2007) Selective incorporation of polyanionic molecules into hamster prions. *J. Biol. Chem. 282*, 36341−36353.

(21) Colby, D. W., Giles, K., Legname, G., Wille, H., Baskakov, I. V., DeArmond, S. J., and Prusiner, S. B. (2009) Design and construction of diverse mammalian prion strains. *Proc. Natl. Acad. Sci. U. S. A. 106*, 20417−20422.

(22) Legname, G., Nguyen, H.-O. B., Baskakov, I. V., Cohen, F. E., DeArmond, S. J., and Prusiner, S. B. (2005) Strain-specified characteristics of mouse synthetic prions. *Proc. Natl. Acad. Sci. U. S. A. 102*, 2168−2173.

(23) Sun, Y., Makarava, N., Lee, C. I., Laksanalamai, P., Robb, F. T., and Baskakov, I. V. (2008) Conformational stability of PrP amyloid firbils controls their smallest possible fragment size. *J. Mol. Biol. 376*, 1155−1167.

(24) Peretz, D., Williamson, R. A., Legname, G., Matsunaga, Y., Vergara, J., Burton, D., DeArmond, S., Prusiner, S., and Scott, M. R. (2002) A Change in the Conformation of Prions Accompanies the Emergence of a New Prion Strain. *Neuron 34*, 921−932.

(25) Ayers, J. L., Schutt, C. R., Shikiya, R. A., Aguzzi, A., Kincaid, A. E., and Bartz, J. C. (2011) The strain-encoded relationship between PrP replication, stability and processing in neurons is predictive of the incubation period of disease. *PLoS Pathog. 7*, e1001317.

(26) Petkova, A. T., Leapman, R. D., Gua, Z., Yau, W.-M., Mattson, M. P., and Tycko, R. (2005) Self-Propagating, Molecular-Level Polymorphism in Alzheimer's b-Amyloid fibrils. *Science 307*, 262−265.

(27) Lee, Y. J., Savtchenko, R., Ostapchenko, V. G., Makarava, N., and Baskakov, I. V. (2011) Molecular Structure of Amyloid Fibrils Controls the Relationship between Fibrillar Size and Toxicity. *PLoS One 6*, e20244.

(28) Abid, K., Morales, R., and Soto, C. (2010) Cellular factors implicated in prion replication. *FEBS Lett. 584*, 2409−2314.

(29) Kraft, C., Deplazes, A., Sohrmann, M., and Peter, M. (2008) Mature ribosomes are selectively degraded upon starvation by an autophagy pathway requiring the Ubp3p/Bre5p ubiquitin protease. *Nat. Cell Biol. 10*, 602−610.

(30) Yokoyama, T., Takeuchi, A., Yamamoto, M., Kitamoto, T., Ironside, J. W., and Morita, M. (2011) Heparin enhances the cell-protein misfolding cyclic amplification efficiency of variant Creutzfeldt-Jakob disease. *Neroscience Lett.*, in press.